A ROBUST AND SCALABLE METHOD WITH AN ANALYTIC SOLUTION FOR MULTI-SUBJECT FMRI DATA ANALYSIS

Trung Vu[a], Hanlu Yang[a*], Francisco Laport[a,b], Ben Gabrielson[a], Vince D. Calhoun[c], and Tülay Adalı[a]*

[a] Department of CSEE, University of Maryland, Baltimore County, MD 21250, USA
[b] CITIC Research Center, University of A Coruña, Campus de Elviña, 15071 A Coruña, Spain
[c] TReNDS, Georgia State University, Georgia Institute of Technology, and Emory University, Atlanta, GA 30303, USA
{trungvv, hyang3, flopez2, bengabr1, adali}@umbc.edu vcalhoun@gsu.edu

ABSTRACT

Joint blind source separation (JBSS) is a powerful framework for extracting latent sources from multiple datasets while keeping their coherence across multiple linked datasets. Algorithms for JBSS, while offering the capability of improved estimation performance, often incur high computational complexity and hence are not scalable to studies with hundreds or thousands of datasets. In this paper, we propose a simple yet efficient method for source separation that exploits both the correlation among sources within each dataset and across the datasets. The proposed method, named reference-guided component analysis (RGCA), uses source templates as references to (i) guide the separation of sources on each dataset and (ii) establish source dependence and automatically align them across the datasets. In addition, we promote independence among latent sources within each dataset by adding orthogonal constraints on the demixing vectors. The resulting optimization admits an analytic solution that enables extremely fast implementation of RGCA. Our numerical results demonstrate that RGCA obtains competitive performance while having a runtime far superior to other JBSS methods. The proposed method provides a robust and scalable solution to multi-subject functional magnetic resonance imaging (fMRI) studies, enabling joint analysis of thousands of subjects within a few minutes.

***Index Terms*—** blind source separation, constrained latent variable analysis, multi-subject fMRI analysis.

1. INTRODUCTION

Blind source separation (BSS) is the problem of recovering a set of source signals from a mixture of signals, without prior knowledge about the sources or the mixing process. When multiple datasets are analyzed as a group, joint blind source separation (JBSS) can improve upon BSS by exploiting the statistical dependence among latent sources across the datasets. Example applications of JBSS include the joint analysis of multi-subject data in medical studies [1–4] or the separation of speech and audio signals in multiple frequency bands [5–8]. In such problems, along with the correspondence of the sources within each subject/frequency band, there is often a strong dependence among latent sources across multiple subjects/frequency bands. The JBSS framework can leverage this additional diversity to obtain better performance compared with BSS applied to individual datasets separately.

A widely-used JBSS method is group ICA [1], which concatenates the datasets and applies principal component analysis (PCA) followed by independent component analysis (ICA) to extract group independent components (IC). These ICs can then be used to compute the subject-specific components by back-reconstruction, using dual or other flavors of regression. Nonetheless, group ICA assumes that there is a common subspace among all datasets and hence, its ability to capture the variability across datasets can be limited [9]. Another powerful approach to JBSS is independent vector analysis (IVA), which generalizes ICA by exploiting the statistical dependencies across datasets [10, 11]. By modeling the corresponding sources across datasets (grouped into a "source component vector" or SCV) with a multivariate distribution, IVA can exploit the statistical dependence within each SCV and thus better model and exploit the variability in the data [12, 13]. The disadvantage of IVA, however, is the high computational cost such that it quickly becomes intractable as the number of datasets increases. Recently, Gabrielson *et al.* [14] introduced IVA regression (regIVA) as an efficient method to extend an IVA-based model to a large-scale JBSS. Starting with a manageably small subset of the datasets, regIVA estimates regressor sources from the subset that capture variability across the datasets and then estimates sources in the remaining datasets using multilinear regression. It has been demonstrated in [14] that regIVA retains very similar source separation performance to the computationally expensive IVA algorithm. Nonetheless, there are no guarantees of independence among the sources within each dataset since the regressed sources are estimated separately from each other.

JBSS methods can be improved in various ways by leveraging prior knowledge about the sources or the mixing matrices. In the early stages, a simple model-based method for task-related functional magnetic resonance imaging (fMRI) data analysis, the general linear model (GLM) [15, 16], uses user-defined mixing matrices to regress the spatial maps. Since this approach relies solely on the specification of the mixing matrices, it is sensitive to each problem setting and does not take into account the variability in different datasets. Importantly, the GLM cannot be applied to resting-state fMRI data, a dominant type of data recently, since there is no specification of time course models. Another more attractive approach is using rough templates of the sources [17, 18] or the mixing matrix [19, 20] as constraints in optimizing the cost function. A reliable set of references guides the optimization to avoid sub-optimal solutions and increase the quality of source separation. Examples of reference-constrained methods for source separation are constrained ICA [21, 22] and constrained IVA [23, 24]. However, these methods inherit the drawback of their unconstrained versions, e.g., the lack of capturing the variability for group ICA or the high computational cost for IVA. Thus, there is a need for a constrained method that is able to capture the variability across datasets while being computationally inexpensive.

* Trung Vu and Hanlu Yang contributed equally to this work.

This work is supported in part by the grants NIH R01MH118695, NIH R01MH123610, NIH R01AG073949, NSF 2316420, and Xunta de Galicia ED481B 2022/012.

In this paper, we propose a simple yet efficient method for source separation of multiple datasets that uses source templates as references. The proposed method, named reference-guided component analysis (RGCA), simultaneously considers two objectives: (i) best approximating the data using the references, and (ii) enforcing the independence among latent sources within each dataset by adding orthogonal constraints on the demixing vectors. The resulting optimization admits an analytic solution that enables extremely efficient implementation of RGCA. Our numerical results demonstrate that RGCA obtains competitive performance while having a runtime far superior to other JBSS methods. The proposed method offers a robust and scalable solution to group fMRI studies, enabling joint analysis of thousands of subjects within a few minutes. The rest of this paper is organized as follows. Section 2 provides a brief overview of the background of JBSS. Then, our proposed method is described in Section 3, followed by numerical results that demonstrate the performance of different JBSS algorithms for simulated fMRI-like data in Section 4.

2. PRELIMINARIES

Notation: Throughout the paper, we use boldfaced symbols to denote vectors and matrices, while the elements of a vector/matrix are unbold. The notation $(\cdot)^\top$ denotes the transpose of a matrix. In addition, $\boldsymbol{I}_n$ denotes the $n \times n$ identity matrix and $\boldsymbol{0}_{m\times n}$ denotes the $m \times n$ matrix of all zeros. Given an n-dimensional vector $\boldsymbol{x}$, x_i denotes its ith element and $\mathrm{diag}(\boldsymbol{x})$ denotes the $n \times n$ diagonal matrix with the corresponding diagonal entries $x_1, \ldots, x_n$.

Consider K datasets, each formed by V samples of linear mixtures of N independent sources

$$\boldsymbol{x}^{[k]}(v) = \boldsymbol{A}^{[k]}\boldsymbol{s}^{[k]}(v), \tag{1}$$

for $k = 1, \ldots, K$ and $v = 1, \ldots, V$. Here, $\boldsymbol{A}^{[k]} \in \mathbb{R}^{P\times N}(P \geq N)$ is an unknown mixing matrix with full column rank and $\boldsymbol{s}^{[k]}(v) = [s_1^{[k]}(v), \ldots, s_N^{[k]}(v)]^\top$ is the vth sample of the corresponding source vector of the kth dataset. In its matrix form, (1) can be represented as $\boldsymbol{X}^{[k]} = \boldsymbol{A}^{[k]}\boldsymbol{S}^{[k]}$, where $\boldsymbol{X}^{[k]} = [\boldsymbol{x}^{[k]}(1), \ldots, \boldsymbol{x}^{[k]}(V)] \in \mathbb{R}^{P\times V}$ and $\boldsymbol{S}^{[k]} = [\boldsymbol{s}^{[k]}(1), \ldots, \boldsymbol{s}^{[k]}(V)] \in \mathbb{R}^{N\times V}$. The goal of JBSS is to recover the original source components $\boldsymbol{S}^{[k]}$ from the mixture signals $\boldsymbol{X}^{[k]}$, for all $k = 1, \ldots, K$. When applying JBSS to multi-subject fMRI analysis, each dataset often corresponds to one subject with source matrices corresponding to subject-specific networks and mixing matrices corresponding to their associated time courses.

In the estimation of the source components, it is convenient to introduce the concept of source component vector (SCV). By stacking the nth source component across K datasets, the nth SCV is defined as a K-dimensional random vector $\boldsymbol{s}_n = [s_n^{[1]}, \ldots, s_n^{[K]}]^\top$. An appropriate multivariate probability density function (pdf) of the SCV can take all order statistical information within and across the K datasets into account. Additionally, we define demixing matrices of form $\boldsymbol{W}^{[k]} = [\boldsymbol{w}_1^{[k]}, \ldots, \boldsymbol{w}_N^{[k]}]^\top \in \mathbb{R}^{N\times P}$. One common assumption in blind source separation is that the underlying sources are mutually statistically independent, which enables identifiability up to permutation and scaling ambiguities. This implies that if the data matrix $\boldsymbol{X}$ is standardized and pre-whitened, i.e., $\boldsymbol{X}\boldsymbol{X}^\top = V\boldsymbol{I}_P$, then the corresponding mixing (or demixing) matrix $\boldsymbol{A}$ (or $\boldsymbol{W}$) has approximately orthonormal columns (or rows) [25], which is the motivation of our proposed algorithm in the next section.

3. REFERENCE-GUIDED COMPONENT ANALYSIS

This section describes our proposed algorithm for source separation using reference signals as prior information. We leverage the references to guide the separation of sources in each dataset separately. This promotes a simple analytic solution for individual datasets while effectively retaining the source dependence across datasets via the common use of reference guidance. As a by-product, the proposed algorithm automatically aligns source components across datasets since each component is associated with only one reference signal. In the following, we present our reference-guided approach to separating sources in a single dataset.

Given a whitened dataset $\boldsymbol{X} \in \mathbb{R}^{P\times V}$ and the reference signals $\boldsymbol{R} \in \mathbb{R}^{M\times V}$, we aim to find a semi-orthogonal demixing matrix $\boldsymbol{W}$ that maps $\boldsymbol{X}$ to $\boldsymbol{R}$:

$$\min_{\boldsymbol{W}\in\mathbb{R}^{M\times P}} \frac{1}{2V}\|\boldsymbol{R} - \boldsymbol{W}\boldsymbol{X}\|_F^2 \qquad \text{s.t. } \boldsymbol{W}\boldsymbol{W}^\top = \boldsymbol{I}_M, \tag{2}$$

where $\|\cdot\|_F$ denotes the Frobenius norm of a matrix. As mentioned earlier, the orthogonal constraint on $\boldsymbol{W}$ facilitates the uncorrelatedness among the estimated sources. At the same time, minimizing the distance between the sources and the references provides a better model match such as statistical properties of the sources. Problem (2) is well-known as the orthogonal Procrustes problem [26], which is equivalent to finding the nearest orthogonal matrix to $\boldsymbol{R}\boldsymbol{X}^\top$. Let $\boldsymbol{R}\boldsymbol{X}^\top = \boldsymbol{U}\boldsymbol{\Sigma}\boldsymbol{V}^\top$ be the singular value decomposition (SVD) such that $\boldsymbol{U} \in \mathbb{R}^{M\times M}$ and $\boldsymbol{V} \in \mathbb{R}^{P\times P}$ are orthogonal matrix, and $\boldsymbol{\Sigma} \in \mathbb{R}^{M\times P}$ with diagonal entries being the singular values of $\boldsymbol{R}\boldsymbol{X}^\top$. It can be shown that (2) admits a closed form solution given by $\hat{\boldsymbol{W}} = \boldsymbol{U}\boldsymbol{V}^\top$.

In many real-world applications, the orthogonal constraint is often too strict and one would like to relax it in order to obtain a more practical solution. That motivates the following regularized version of (2):

$$\min_{\boldsymbol{W}\in\mathbb{R}^{M\times P}} \frac{1}{2V}\|\boldsymbol{R} - \boldsymbol{W}\boldsymbol{X}\|_F^2 + \frac{\lambda}{4}\left\|\boldsymbol{W}\boldsymbol{W}^\top - \boldsymbol{I}_M\right\|_F^2, \tag{3}$$

where $\lambda > 0$ is a regularization parameter that controls how close $\boldsymbol{W}$ is to a semi-orthogonal matrix. Let $f(\boldsymbol{W})$ be the objective function in (3). The gradient of f is given by

$$\begin{aligned}\nabla f(\boldsymbol{W}) &= \frac{1}{V}(\boldsymbol{W}\boldsymbol{X} - \boldsymbol{R})\boldsymbol{X}^\top + \lambda(\boldsymbol{W}\boldsymbol{W}^\top - \boldsymbol{I}_M)\boldsymbol{W} \\ &= \lambda\boldsymbol{W}\boldsymbol{W}^\top\boldsymbol{W} + (1-\lambda)\boldsymbol{W} - \frac{1}{V}\boldsymbol{R}\boldsymbol{X}^\top. \end{aligned}\tag{4}$$

In the last equality, we use the fact that the data is whitened. Setting the derivative $\nabla f(\boldsymbol{W})$ to $\boldsymbol{0}$, we obtain an analytic solution for (3) as follows. Let $\frac{1}{V}\boldsymbol{R}\boldsymbol{X}^\top = \boldsymbol{U}\boldsymbol{\Sigma}\boldsymbol{V}^\top$ and $\boldsymbol{W} = \boldsymbol{U}_{\boldsymbol{W}}\boldsymbol{\Sigma}_{\boldsymbol{W}}\boldsymbol{V}_{\boldsymbol{W}}^\top$ be the SVDs of the corresponding matrices. Substituting the SVDs back into (4), we obtain

$$\nabla f(\boldsymbol{W}) = \boldsymbol{U}_{\boldsymbol{W}}\big(\lambda\boldsymbol{\Sigma}^3 + (1-\lambda)\boldsymbol{\Sigma}\big)\boldsymbol{V}_{\boldsymbol{W}}^\top - \boldsymbol{U}\boldsymbol{\Sigma}\boldsymbol{V}^\top.$$

Due to the uniqueness of the SVD, $\nabla f(\boldsymbol{W}) = \boldsymbol{0}$ is equivalent to $\boldsymbol{U}_{\boldsymbol{W}} = \boldsymbol{U}$, $\boldsymbol{V}_{\boldsymbol{W}} = \boldsymbol{V}$, and for $i = 1, \ldots, M$:

$$\lambda\big(\sigma_i(\boldsymbol{W})\big)^3 + (1-\lambda)\sigma_i(\boldsymbol{W}) - \sigma_i(\boldsymbol{R}\boldsymbol{X}^\top) = 0, \tag{5}$$

where $\sigma_i(\boldsymbol{W})$ denotes the ith largest singular value of $\boldsymbol{W}$.

Lemma 1. *The depressed cubic equation (5), w.r.t. $\sigma_i(\boldsymbol{W})$, has exactly one real positive root for any $\lambda > 0$.*

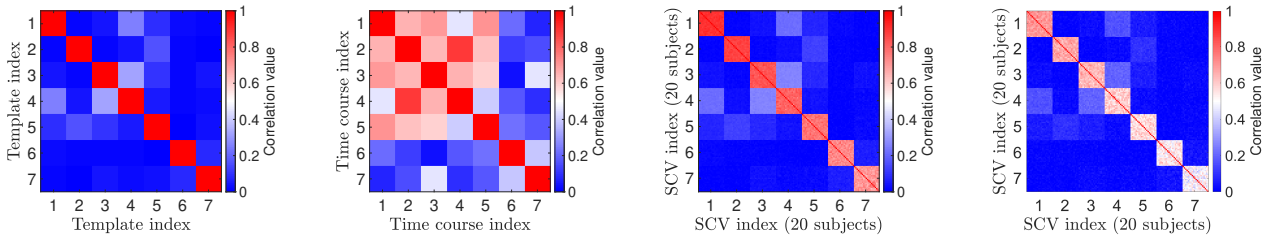

(a) Template covariance matrix (b) Sample time course correlation (c) SCV — Low variability (d) SCV — High variability

Fig. 1: Visualization of (a) the covariance matrix of the template sources (with $N = 7$ and $V = 57878$), (b) an example of the correlation among the time courses used to mix the sources (with $P = 10$), and the full SCV covariance matrices generated based on (7) in (c) low variability case with $\varphi \in [0.1, 0.3]$ and (d) high variability case with $\varphi \in [0.3, 0.5]$.

Algorithm 1: Reference-Guided Component Analysis (RGCA)

Input: $\boldsymbol{X} \in \mathbb{R}^{P\times V}, \boldsymbol{R} \in \mathbb{R}^{M\times V}, \lambda > 0$
Output: $\boldsymbol{W} \in \mathbb{R}^{M\times P}, \boldsymbol{A} \in \mathbb{R}^{P\times M}$
1: Compute $\boldsymbol{Q} = \frac{1}{V}\boldsymbol{R}\boldsymbol{X}^\top$ ▷ $\mathcal{O}(MPV)$
2: Perform the SVD $\boldsymbol{Q} = \boldsymbol{U}\boldsymbol{\Sigma}\boldsymbol{V}^\top$ ▷ $\mathcal{O}(M^2P)$
3: **for** $i = 1 : M$ **do**
4: Solve the depressed cubic equation (5) to find the unique real positive root $\sigma_i(\boldsymbol{W})$ ▷ $\mathcal{O}(1)$
5: $\boldsymbol{W} = \boldsymbol{U}\,\mathrm{diag}(\sigma_1(\boldsymbol{W}), \ldots, \sigma_M(\boldsymbol{W}))\boldsymbol{V}^\top$ ▷ $\mathcal{O}(M^2P)$
6: $\boldsymbol{A} = \boldsymbol{W}^\top(\boldsymbol{W}\boldsymbol{W}^\top)^{-1}$ ▷ $\mathcal{O}(M^2P)$

The proof of this lemma is a straightforward consequence of Vieta's formulas [27] and is omitted in this paper due to space limitation. We summarize the new algorithm, Reference-Guided Component Analysis (RGCA) in Algorithm 1. When K datasets are available, one can apply RGCA to each dataset separately. The overall complexity of the algorithm is $\mathcal{O}(KMPV + KM^2P)$.

Remark 1. *An alternative formulation of (3) is given by*

$$\min_{\boldsymbol{A}\in\mathbb{R}^{P\times M}} \frac{1}{2V}\left\|\boldsymbol{X} - \boldsymbol{A}\boldsymbol{R}\right\|_F^2 + \frac{\lambda}{4}\left\|\boldsymbol{A}^\top\boldsymbol{A} - \boldsymbol{I}_M\right\|_F^2. \quad (6)$$

In this view, we aim to find a semi-orthogonal mixing matrix $\boldsymbol{A}$ that maps $\boldsymbol{R}$ to $\boldsymbol{X}$. While the analytic solutions differ in general, we observe the two formulations yield similar performance in practice.

4. NUMERICAL RESULTS

This section compares the performance of the proposed method with other reference-constrained algorithms for JBSS using simulated fMRI-like data. Our goal is to better understand the behavior of these algorithms in various settings of fMRI datasets.

4.1. Hybrid Data Setup

Extraction of template sources. We use reference signals extracted by NeuroMark, i.e., the Neuromark_fMRI_1.0 template [28], which includes 53 fMRI networks and is divided into seven functional domains based on their anatomical and functional properties: the subcortical (SC), auditory (AUD), sensorimotor (MOT), visual (VIS), cognitive control (CC), default mode (DMN) and cerebellar (CB) domains. In the hybrid simulation experiment with varying numbers of datasets, to reduce the runtime, we only use a subset of $N = 7$ templates (with 5 from SC and 2 from AUD). For convenience, we denote the set of N template sources by $\{\boldsymbol{r}_n\}_{n=1}^N$, each containing $V = 57878$ samples with zero mean and unit variance. Figure 1-(a) shows the correlation among the template sources. Due to the nature of real fMRI sources, there is a certain level of dependency among the templates, i.e., they are not absolutely independent.

Hybrid source generation. Given N template sources, we generate V observations of SCVs $\{\boldsymbol{S}_n\}_{n=1}^N \subset \mathbb{R}^{K\times V}$ for K datasets as follows. First, we define a NK-dimensional random vector $\boldsymbol{z} = [\boldsymbol{z}_1^\top, \ldots, \boldsymbol{z}_N^\top]^\top$ following a multivariate Gaussian distribution (MGD) with zero mean and covariance matrix $\mathbb{E}[\boldsymbol{z}\boldsymbol{z}^\top] = \mu\boldsymbol{Q}\boldsymbol{Q}^\top + (1-\mu)\,\mathrm{blkdiag}\{\boldsymbol{Q}_n\boldsymbol{Q}_n^\top\}_{n=1}^N$, where the rows of $\boldsymbol{Q} \in \mathbb{R}^{NK\times NK}$ are iid uniformly distributed on the unit sphere in $\mathbb{R}^{NK}$ and $\mu > 0$ controls the correlation across different sources. Here $\mathrm{blkdiag}\{\boldsymbol{Q}_n\boldsymbol{Q}_n^\top\}_{n=1}^N$ is a $NK\times NK$ block diagonal matrix formed by N square matrices $\boldsymbol{Q}_n \in \mathbb{R}^{K\times K}$ whose rows are iid uniformly distributed on the unit sphere in $\mathbb{R}^K$. Next, we use $\boldsymbol{z}$ to generate V samples of the multivariate noise and partitioning the sample matrix into N submatrices of dimension $K \times V$, i.e., $\boldsymbol{Z} = [\boldsymbol{Z}_1^\top, \ldots, \boldsymbol{Z}_N^\top]^\top$. The nth source data matrix is formed by adding the multivariate noise $\boldsymbol{Z}_n$ to the template $\boldsymbol{r}_n$

$$\boldsymbol{S}_n = \sqrt{1-\varphi_n^2}\mathbf{1}_K\boldsymbol{r}_n^\top + \varphi_n\boldsymbol{Z}_n \quad \in \mathbb{R}^{K\times V}, \quad (7)$$

where $\varphi_n \in [0, 1]$ controls how close the nth source is to the reference $\boldsymbol{r}_n$. Figures 1-(c) and (d) depict the SCV covariance matrices of the simulated fMRI-like data corresponding to two scenarios: (i) low variability ($\varphi \in [0.1, 0.3]$), and (iii) high variability ($\varphi \in [0.3, 0.5]$). Third, for each of the K datasets, we generate a rectangular mixing matrix $\boldsymbol{A}^{[k]} \in \mathbb{R}^{P\times N}$, for $P \geq N$ being the number of mixtures, that represents the time courses for different brain components. The correlation between two time courses within the same domain, e.g., SC or AUD, is higher than the one across different domains. Figure 1-(b) shows the block structure of the time-course covariance matrix, which reflects the functional domains of the templates (e.g., 5 sources from SC and 2 sources from AUD). Finally, the mixture data for each dataset is created by adding white noise to the mixture

$$\boldsymbol{X}^{[k]} = \boldsymbol{A}^{[k]}\boldsymbol{S}^{[k]} + \boldsymbol{H} \in \mathbb{R}^{P\times V}, \quad k = 1, \ldots, K,$$

where the entries of $\boldsymbol{H} \in \mathbb{R}^{P\times V}$ are normally distributed $\mathcal{N}(0, \sigma^2)$. The reference signals are taken as M out of the N source templates, where we consider two cases $M = 7$ (fully referenced) and $M = 5$ (partially referenced) in our simulation. In the latter case when $M = 5$, we remove one reference from SC and one reference from AUD.

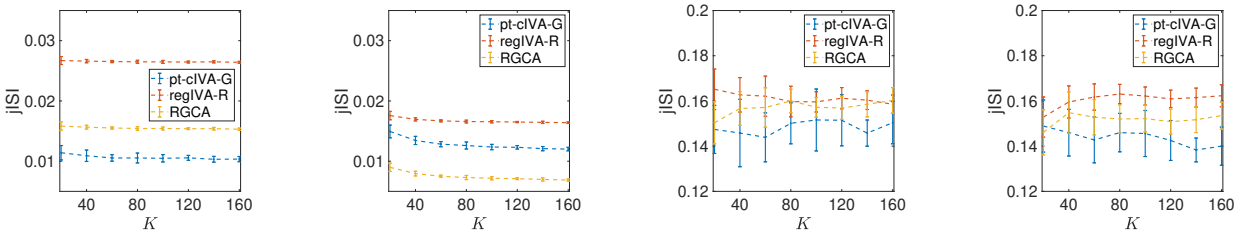

(a) $\varphi \in [0.1, 0.3]$ and $M = 7$ (b) $\varphi \in [0.3, 0.5]$ and $M = 7$ (c) $\varphi \in [0.1, 0.3]$ and $M = 5$ (d) $\varphi \in [0.3, 0.5]$ and $M = 5$

Fig. 2: Four scenarios of the simulated fMRI-like data with $N = 7$, $P = 10$, $V = 57878$, and $\mu = 0.3$ as the number of datasets K increases: (a) low variability and fully referenced, (b) high variability and fully referenced, (c) low variability and partially referenced, and (d) high variability and partially referenced. The error bars represent one standard deviation calculated over 20 runs.

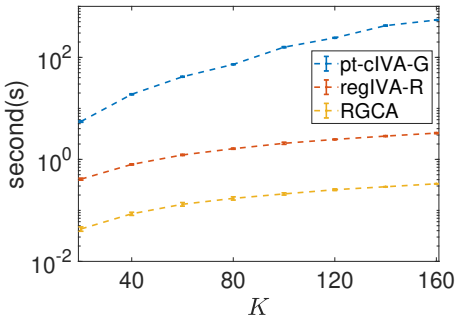

Fig. 3: Runtime of three compared algorithm in second(s).[1] pt-cIVA-G is the slowest method as its computational complexity increases quadratically with the number of datasets K. While the complexity of both regIVA-R and RGCA is linear in K, we highlight that the proposed RGCA is almost 20 times faster than regIVA-R.

4.2. Compared Methods

We compare our proposed RGCA method with pt-cIVA [24] and a reference regression based on regIVA [14], which we call "regIVA-R". In [24], the authors introduce pt-cIVA for Laplace-distributed sources that have a better model match for fMRI data but with a very high computational cost. In this simulation, we implement a faster Gaussian version, named pt-cIVA-G, that is more suitable for experiments with large numbers of datasets. On the other hand, regIVA is a fast method since it admits an analytic solution. We note that the original approach in [14] is fully blind and more general, using SCVs estimated from a subset of the datasets to estimate sources in the remaining datasets. In our context, regIVA-R uses the regIVA cost function but replaces the regressor SCVs with the user-provided references. Finally, for RGCA, we use the regularization value $\lambda = 1$ as it yields a good balance between the two costs in (3).

In our simulations, we use the joint inter-symbol-interference (jISI) [29] as the metric to compare the separation performance of JBSS methods when the true mixing matrices are known. This is a normalized score between 0 and 1 that measures how close the estimates are to true mixing matrices subject to permutation and scaling. Thus, the jISI metric penalizes SCV estimates that are not consistently aligned across datasets and a score equal to 0 indicates ideal separation performance.

4.3. Results

There are four scenarios considered in our evaluation, corresponding to two levels of variability and two cases for the number of templates used as references (see details in Fig. 2). Overall, pt-cIVA-G (blue dashed line) yields the best performance, followed by RGCA (yellow dashed line) and then regIVA-R (red dashed line). When the variability is low and all templates are used (plot (a)), pt-cIVA-G and RGCA achieve similarly higher jISI than regIVA-R. However, when the variability increases (plot (b)), RGCA captures this trend better and outperforms the other two methods, thanks to the simultaneous exploitation of source templates and the orthogonality of demixing matrices. When only 5 out of 7 templates are used (plots (c) and (d)), we observe that the three algorithms have similar jISI, with pt-cIVA-G achieving the highest score and regIVA-R yielding the lowest score. This can be explained by the fact that pt-cIVA-G inherits the aforementioned powerful properties of the IVA framework while the estimated sources from regIVA-R are not necessarily independent or uncorrelated. It is worthwhile noting that RGCA performs relatively well compared with pt-cIVA-G but has a considerably faster runtime. Figure 3 depicts the outstanding runtime performance of RGCA compared with regIVA-R and pt-cIVA-G. Notably, our algorithm only takes less than half a second to separate 7 sources in 160 datasets with 57878 samples.

5. CONCLUSION

We presented reference-guided component analysis (RGCA) as an efficient method for source separation with application in multi-subject fMRI data analysis. The proposed method leverages prior information on the sources (templates) as references for the solution and can be solved analytically, facilitating remarkably fast implementation of RGCA. Simulations with hybrid fMRI-like data illustrated the separation capability of RGCA while capturing well the variability among the datasets, compared to prominent JBSS methods. It is promising that the proposed RGCA can be used on real fMRI data with thousands of subjects to obtain insightful results within only a few minutes. Future works will also address how to divide subjects from large-scale datasets into different homogeneous subgroups and perform RGCA on each subgroup separately.

[1]The hardware used in the computational studies is part of the UMBC High Performance Computing Facility (HPCF). See hpcf.umbc.edu for more information on HPCF and the projects using its resources.

6. REFERENCES

[1] Vince D Calhoun, Tülay Adalı, Godfrey D Pearlson, and James J Pekar, "A method for making group inferences from functional MRI data using independent component analysis," *Hum. Brain Mapp.*, vol. 14, no. 3, pp. 140–151, 2001.

[2] Tülay Adalı, Yuri Levin-Schwartz, and Vince D Calhoun, "Multimodal data fusion using source separation: Application to medical imaging," *Proc. IEEE*, vol. 103, no. 9, pp. 1494–1506, 2015.

[3] Xun Chen, Hu Peng, Fengqiong Yu, and Kai Wang, "Independent vector analysis applied to remove muscle artifacts in EEG data," *IEEE Trans. Instrum. Meas.*, vol. 66, no. 7, pp. 1770–1779, 2017.

[4] Chunying Jia, Mohammad ABS Akhonda, Qunfang Long, Vince D Calhoun, Shari Waldstein, and Tülay Adalı, "C-ICT for discovery of multiple associations in multimodal imaging data: application to fusion of fMRI and DTI data," in *Annu. Conf. Inf. Sci. Syst.* IEEE, 2019, pp. 1–5.

[5] Taesu Kim, Hagai T Attias, Soo-Young Lee, and Te-Won Lee, "Blind source separation exploiting higher-order frequency dependencies," *IEEE Trans. Audio Speech Lang. Process.*, vol. 15, no. 1, pp. 70–79, 2006.

[6] Yanfeng Liang, Jack Harris, Syed Mohsen Naqvi, Gaojie Chen, and Jonathon A Chambers, "Independent vector analysis with a generalized multivariate Gaussian source prior for frequency domain blind source separation," *Signal Process.*, vol. 105, pp. 175–184, 2014.

[7] Mehrez Souden, Shoko Araki, Keisuke Kinoshita, Tomohiro Nakatani, and Hiroshi Sawada, "A multichannel MMSE-based framework for joint blind source separation and noise reduction," in *Proc. IEEE Int. Conf. Acoust. Speech Signal Process.* IEEE, 2012, pp. 109–112.

[8] Li Li, Kazuhito Koishida, and Shoji Makino, "Online directional speech enhancement using geometrically constrained independent vector analysis," in *Proc. Annu. Conf. Int. Speech Commun. Assoc.*, 2020, pp. 61–65.

[9] Andrew M Michael, Mathew Anderson, Robyn L Miller, Tülay Adalı, and Vince D Calhoun, "Preserving subject variability in group fMRI analysis: Performance evaluation of GICA vs. IVA," *Front. Syst. Neurosci.*, vol. 8, pp. 106, 2014.

[10] Taesu Kim, Torbjørn Eltoft, and Te-Won Lee, "Independent vector analysis: An extension of ICA to multivariate components," in *Indep. Compon. Anal. Blind Signal Sep.* Springer, 2006, pp. 165–172.

[11] Matthew Anderson, Tülay Adalı, and Xi-Lin Li, "Joint blind source separation with multivariate Gaussian model: Algorithms and performance analysis," *IEEE Trans. Signal Process.*, vol. 60, no. 4, pp. 1672–1683, 2011.

[12] Jonathan Laney, Kelly P Westlake, Sai Ma, Elizabeth Woytowicz, Vince D Calhoun, and Tülay Adalı, "Capturing subject variability in fMRI data: A graph-theoretical analysis of GICA vs. IVA," *J. Neurosci. Methods*, vol. 247, pp. 32–40, 2015.

[13] Qunfang Long, Suchita Bhinge, Vince D Calhoun, and Tülay Adalı, "Independent vector analysis for common subspace analysis: Application to multi-subject fMRI data yields meaningful subgroups of schizophrenia," *NeuroImage*, vol. 216, pp. 116872, 2020.

[14] Ben Gabrielson, Mingyu Sun, Mohammad Abu Baker Siddique Akhonda, Vince D Calhoun, and Tülay Adali, "Independent vector analysis with multivariate Gaussian model: A scalable method by multilinear regression," in *Proc. IEEE Int. Conf. Acoust. Speech Signal Process.* IEEE, 2023, pp. 1–5.

[15] Karl J Friston, Peter Jezzard, and Robert Turner, "Analysis of functional MRI time-series," *Hum. Brain Mapp.*, vol. 1, no. 2, pp. 153–171, 1994.

[16] Vince D Calhoun, Tülay Adali, Vince B McGinty, James J Pekar, Todd D Watson, and Godfrey D Pearlson, "fMRI activation in a visual-perception task: Network of areas detected using the general linear model and independent components analysis," *NeuroImage*, vol. 14, no. 5, pp. 1080–1088, 2001.

[17] Wei Lu and Jagath C Rajapakse, "Approach and applications of constrained ICA," *IEEE Trans. Neural Netw.*, vol. 16, no. 1, pp. 203–212, 2005.

[18] Zhi-Lin Zhang, "Morphologically constrained ICA for extracting weak temporally correlated signals," *Neurocomputing*, vol. 71, no. 7-9, pp. 1669–1679, 2008.

[19] Vince D Calhoun, Tülay Adalı, Michael C Stevens, Kent A Kiehl, and James J Pekar, "Semi-blind ICA of fMRI: a method for utilizing hypothesis-derived time courses in a spatial ICA analysis," *Neuroimage*, vol. 25, no. 2, pp. 527–538, 2005.

[20] Maarten De Vos, Lieven De Lathauwer, and Sabine Van Huffel, "Spatially constrained ICA algorithm with an application in EEG processing," *Signal Process.*, vol. 91, no. 8, pp. 1963–1972, 2011.

[21] Yuhui Du and Yong Fan, "Group information guided ICA for fMRI data analysis," *Neuroimage*, vol. 69, pp. 157–197, 2013.

[22] Hanlu Yang, Trung Vu, Qunfang Long, Vince Calhoun, and Tülay Adali, "Identification of homogeneous subgroups from resting-state fMRI data," *Sensors*, vol. 23, no. 6, pp. 3264, 2023.

[23] Suchita Bhinge, Qunfang Long, Yuri Levin-Schwartz, Zois Boukouvalas, Vince D Calhoun, and Tülay Adalı, "Non-orthogonal constrained independent vector analysis: Application to data fusion," in *Proc. IEEE Int. Conf. Acoust. Speech Signal Process.* IEEE, 2017, pp. 2666–2670.

[24] Suchita Bhinge, Rami Mowakeaa, Vince D Calhoun, and Tülay Adalı, "Extraction of time-varying spatiotemporal networks using parameter-tuned constrained IVA," *IEEE Trans. Med. Imag.*, vol. 38, no. 7, pp. 1715–1725, 2019.

[25] Aapo Hyvärinen and Erkki Oja, "Independent component analysis: Algorithms and applications," *Neural Netw.*, vol. 13, no. 4-5, pp. 411–430, 2000.

[26] Richard Everson, "Orthogonal, but not orthonormal, Procrustes problems," *Adv. Comput. Math.*, vol. 3, no. 4, 1998.

[27] Ėrnest Borisovich Vinberg, *A Course in Algebra*, American Mathematical Society, 2003.

[28] Yuhui Du, Zening Fu, Jing Sui, Shuang Gao, Ying Xing, Dongdong Lin, Mustafa Salman, Anees Abrol, Md Abdur Rahaman, Jiayu Chen, et al., "NeuroMark: An automated and adaptive ICA based pipeline to identify reproducible fMRI markers of brain disorders," *NeuroImage Clin.*, vol. 28, pp. 102375, 2020.

[29] Yi-Ou Li, Tülay Adali, Wei Wang, and Vince D Calhoun, "Joint blind source separation by multiset canonical correlation analysis," *IEEE Trans. Signal Process.*, vol. 57, no. 10, pp. 3918–3929, 2009.